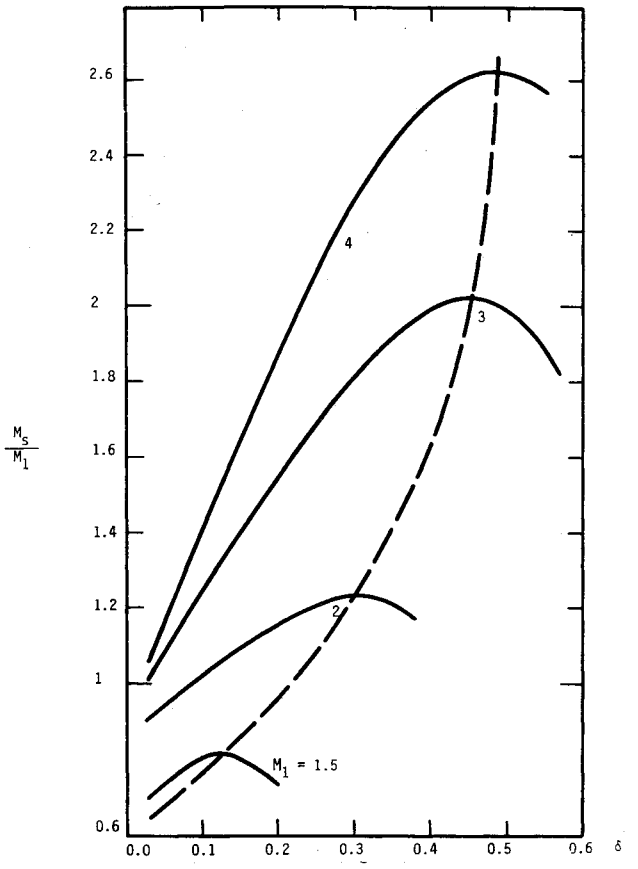

Fig. 3 The ratio of shock formation speed M_s to upstream Mach number M_1 vs wedge semiangle δ (in radians), for various values of M_1. A broken line indicates maximal formation speed. Curves end when an attached shock does not exists (large δ).

tion angles slightly less than the maximum angle for attached shock waves.

Further study of these unsteady formation and cancellation phenomena for the more complex flowfields such as that of Fig. 1 is underway at the present and will be reported in due course.

References

[1]Shapiro, A. H., *The Dynamics and Thermodynamics of Compressible Fluid Flow*, Ronald, New York, 1953, Vols. 1 & 2, p. 1185.

[2]Pope, A., and Goin, K. L., *High Speed Wind Tunnel Testing*, Wiley, New York, 1968, p. 474.

Analysis of ASTM D 3410 Compression Test Specimens

Seng C. Tan*
Wright Materials Research, Dayton, Ohio 45433

Introduction

THE existing compression test methods for composite laminates can be classified into four main categories: end-loaded straight coupon, face-loaded straight coupon, point-loaded sandwich beam, and radial-loaded ring specimen. The methods in the first three categories have been utilized extensively. Unfortunately, the compressive strengths of unidirectional composites measured by different test methods vary significantly.[1-5] The diversity could be attributed to the fact that the stress concentrations in the specimens are significantly different using different test methods. In addition, stability could be a problem for some of the test methods.

Two of the most commonly used compression test methods are the Test Method for Compressive Properties of Unidirectional or Crossply Fiber-Resin Composites (D 3410-87),[6] which are standard test methods utilized by the American Society for Testing and Materials (ASTM). The standard ASTM D 3410 includes the Celanese and the Illinois Institute of Technology Research Institute (IITRI) test methods. The main difference between these two methods is the grip design of the fixtures. The grip construction restricts the overall tabbed specimen thickness of the Celanese test to around 0.157 in. (3.99 mm), whereas the overall tabbed specimen thickness of the IITRI test can be anywhere from 0.059 in. (1.5 mm) to 0.5 in (12.7 mm).

To the author's knowledge, there is no analysis available for the Celanese and the IITRI test methods in the open literature. The small unsupported gauge length of the Celanese and IITRI test specimens [both are 0.5 in. (12.7 mm)] has created a concern that the stress distribution in the specimen may not be uniform. Therefore, the objective of this study is to analyze these compression test specimens.

Formulation

A schematic diagram of the Celanese gripping device is illustrated in Fig. 1. The parameter P denotes the applied load, and R designates the reaction force acting in a ϕ degree direction clockwise from the normal direction of the matching slanted surfaces. The normal and shear load applied at the end tab of the specimen are denoted by N and S, respectively. According to the friction law, the following relation is obtained:

$$\mu = \tan\phi = F/W \tag{1}$$

where μ is the friction coefficient between the contact surfaces. The parameter F is the force required to move one surface over another, and W is the force pressing the surfaces together. The value of μ for clean steel on steel is 0.58 (Ref. 7). Using this value the angle ϕ can be calculated as

$$\phi = \tan^{-1}\mu = 30.11 \text{ deg} \tag{2}$$

Considering the force equilibrium in the vertical direction of Fig. 1a;

$$R = \frac{P}{\sin(10+\phi)} \tag{3}$$

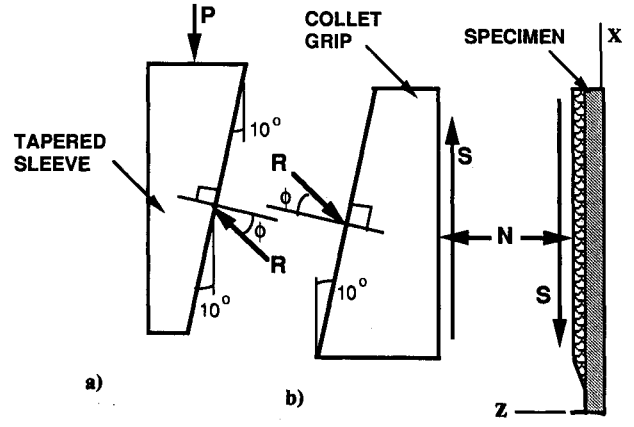

Fig. 1 Load transfer mechanisms between Celanese fixture and specimen.

Received May 31, 1990; revision received June 25, 1990; accepted July 5, 1990.

*Senior Research Scientist (on-site contractor), Air Force Materials Laboratory, WRDC/MLBM, Wright Patterson AFB; currently at Northwestern University, Evanston, IL 60298. Member AIAA.

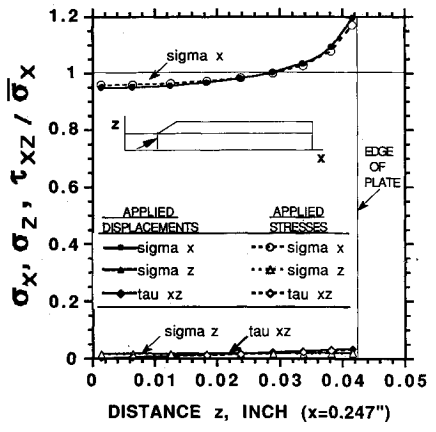

Fig. 2 Stress distribution of an AS4/3504 0-deg Celanese/IITRI specimen.

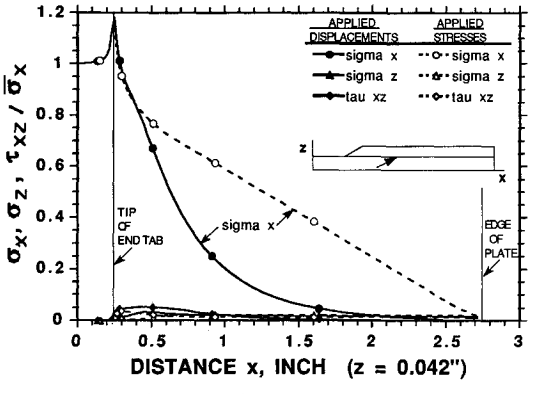

Fig. 3 Stress distribution along the outer surface of a 0-deg Celanese/IITRI specimen.

From Fig. 1b and the force equilibrium conditions, we obtain

$$S = R \sin(10+\phi) = P$$

$$N = R \cos(10+\phi) = 1.187P = 1.187S \tag{4}$$

The ratio of the displacements u and w is different from the ratio of the forces S and N.

The IITRI test method utilizes trapezoidal wedge grips rather than conical wedge grips, which are used for the Celanese test method.[5] Although the gripping devices are somewhat different, the ratios of forces (S and N) that they applied to the specimens are approximately the same. Therefore, a same ratio of stresses (or displacements) can be used for the Celanese and IITRI specimens.

Stress Analysis

A Celanese specimen is 5.5 in. long × 0.25 in. wide (139.7 × 6.35 mm), and the gauge length is 0.5 in. (12.7 mm). The gauge length and the total length of an IITRI specimen are the same as those for the Celanese specimen. Because of the symmetry of the specimen and the loading condition, we only need to model one-fourth of the specimen, as shown in Fig. 1 with an edge view. In this study a two-dimensional plane stress, quadrilateral, isoparametric, finite element method has been chosen for the analysis. Either stress or displacement boundary conditions can be applied. The stress or displacement boundary conditions were applied at the tabs of the specimen. They are described in more detail in the following.

Uniform stress boundary conditions

Along end tab surfaces: applied shear stress τ_{xz}, and normal stress σ_z, *where* $\sigma_z = 1.187\tau_{xz}$.
Along midplane $(0,z)$: applied $u = 0$, $\tau_{xz} = 0$.
Along midplane $(x,0)$: applied $w = 0$, $\tau_{xz} = 0$.
Along the other surfaces: applied $\sigma_z = \tau_{xz} = 0$.

Uniform displacement boundary conditions

Along end tab surfaces: applied displacements u and w.
Along midplane $(0,z)$: applied $u = 0$, $\tau_{xz} = 0$.
Along midplane $(x,0)$: applied $w = 0$, $\tau_{xz} = 0$.
Along the other surfaces: applied $\sigma_z = \tau_{xz} = 0$.

The ratio of the displacements u and w is not the same as the ratio of the stresses (or forces) applied because the stiffnesses of the laminate along the x axis and the z axis is different. The ratio of the applied displacements can be estimated by examining the displacements resulting from the applied uniform stress boundary conditions. The solution of displacements should be nonuniform under uniform stress boundary conditions. Therefore, a few steps of adjustment for the displacements are needed to obtain the appropriate ratio of the stresses given earlier.

Results

The graphite/epoxy AS4/3502 has been selected for the Celanese and IITRI specimens, and the end tab is glass/epoxy $[0/90]_n$. The adhesive properties reported in Ref. 8 were used for this analysis. The mechanical properties of the materials are summarized in Table 1. The thickness of the untabbed region of the specimens being studied here is 0.085 in. (2.159 mm), and the thickness of the end tab is 0.068 in. (1.727 mm). The finite element mesh that is used for this analysis contains 971 elements and 1047 nodes. The through-the-thickness directions of the specimen, adhesive, and end tab contain 8, 3, and 12 elements, respectively. Along the x axis, the respective untabbed and tabbed sections of the specimen contain 15 and 37 divisions.

The results of the stress distributions are plotted along two laminate sections, as shown in the subfigure of Figs. 2 and 3. In Figs. 2 and 3, $\bar{\sigma}_x$ represents the average of the normal stress, σ_x, across the midplane $(0,z)$. The average normal stress $\bar{\sigma}_x$ is calculated by the total applied shear force at the end tab divided by the cross-sectional area of the untabbed region of the specimen. The stresses are very uniform along the midplane $(0,z)$ of the specimen, and the difference between the stresses obtained by uniform stress and uniform displacement boundary conditions is negligible. The stress components σ_z and τ_{xz} are four to five orders of magnitude less than σ_x. Along the laminate section indicated by the subfigure of Fig. 2, the solutions of σ_x obtained by the two applied boundary conditions are approximately the same. The stresses σ_z and τ_{xz}, again, can be disregarded.

Along the laminate section between the specimen and the end tab (Fig. 3), the differences of the stress distributions due to the different boundary conditions are remarkable under the end tab region. Within the gauge length section and the neighborhood of the tab tip, the σ_x obtained from the two different boundary conditions are the same. Therefore, different boundary conditions applied at the end tab only affect the stress distributions under the end tab region of the Celanese specimen. For a thicker specimen of IITRI test, the discrepancy between the stress concentrations obtained by the two different boundary conditions increases.

Summary and Discussion

The stress-strain distributions of the Celanese and IITRI compression specimens have been analyzed using a quadrilateral, isoparametric, finite element method. The load transfer mechanism from the grips to the specimen was evaluated using a strength of materials approach. Both the uniform displace-

ment and the uniform stress boundary conditions were considered at the end tab surfaces. The results under the two different boundary conditions are practically the same within the gauge length section and around the tab tip. Under the end tab region different boundary conditions (stress vs displacement) result in significantly different results. For a thicker IITRI specimen the stress concentrations and the stress profiles obtained by the two different boundary conditions are considerably different. Since there is no stress concentration in the gauge length section of the specimen, the compressive modulus can be measured using the Celanese or IITRI specimens. However, a preliminary study has shown that the apparent strengths determined by these test methods are significantly lower than those obtained from face-supported specimens.[9] This suggests that stability could be a problem for the Celanese and IITRI specimens. Additional stability analysis is needed to confirm this result.

Acknowledgment

This work is supported by the Materials Laboratory of Wright Patterson Air Force Base under contract F33615-88-C-5420.

References

[1]Woolworth, D. H., Curtis, A. R., and Haresceugh, R. I., "A Comparison of Test Techniques Used for the Evaluation of the Unidirectional Compressive Strength of Carbon Fibre-Reinforced Plastic," *Composites*, Oct. 1981, pp. 275–280.

[2]Hofer, K. E., Jr., and Rao, P. N., "A New Static Compression Fixture for Advanced Composite Materials," *Journal of Testing and Evaluation*, Vol. 5, No. 4, 1977, pp. 278–283.

[3]Westberg, R. L., and Abdallah, M. G., "An Experimental and Analytical Evaluation of Three Compressive Test Methods for Unidirectional Graphite/Epoxy Composites," *Proceedings of the 6th International Congress on Experimental Mechanics*, Vol. 1, Portland, OR, June 6–10, 1988, pp. 350–361.

[4]Clark, R. K., and Lisagor, W. B., "Compression Testing of Graphite/Epoxy Composite Materials," *Test Methods and Design Allowables for Fibrous Composites*, edited by C. C. Chamis, American Society for Testing and Materials, ASTM STP 734, 1981, pp. 34–53.

[5]Kim, R. Y., and Tsai, S. W., "A Compressive Test Method for Ring Specimens," *33rd International SAMPE Symposium*, Anaheim, CA, 1988, pp. 1159–1168.

[6]"Standard Test Method for Compressive Properties of Unidirectional or Crossply Fiber-Resin Composites," American Society for Testing and Materials, ASTM D 3410-87, Philadelphia, PA, 1987.

[7]*CRC Handbook of Chemistry and Physics*, 67th ed., CRC, Boca Raton, FL, 1986–87.

[8]Whitney, J. M., and Knight, M., "Effect of Residual Stresses on Edge Delamination in Composite Materials" *Proceedings of the AIAA/ASME/ASCE/AHS/ASC 30th Structures, Structural Dynamics, and Materials Conference*, AIAA, Washington, DC, 1989, pp. 1666–1670.

[9]Tan, S. C., "Effective Stress Fracture Models for Unnotched and Notched Multidirectional Laminates," *Journal of Composite Materials*, Vol. 22, No. 4, 1988, pp. 322–340.

Errata

Numerical Simulation of the Convective Instability in a Dump Combustor

Habib N. Najm and Ahmed F. Ghnoniem
Massachusetts Institute of Technology, Cambridge, Massachusetts 02139

[AIAA Journal 29(6), pp. 911–919 (1991)]

FIGURE 7b was inadvertently omitted from this paper and should have appeared with Fig. 7a as follows.

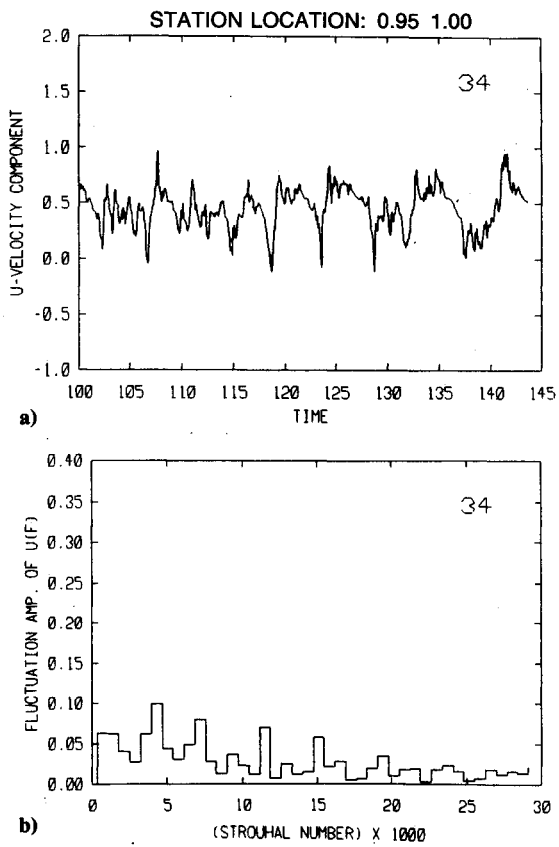

Fig. 7 Velocity fluctuation a) and frequency spectrum b) for cavity with $L/D = 2.0$, $L/\theta_0 = 1000$ at $x/D = 0.95$, $y/D = 1.0$.